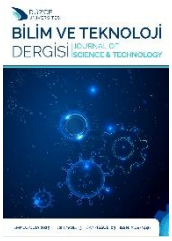

Düzce University
Journal of Science & Technology

Research Article

DFT studies of 2-oxo-2-phenylethyl 3-nitroso-2-phenylimidazo[1,2-a] pyridine-8-carboxylate compound

Cemile BAYDERE DEMİR [a,*]

[a] *FİZYOTERAPİ Programı, SAĞLIK HİZMETLERİ MESLEK Yüksekokulu, Demiroğlu Bilim Üniversitesi, İstanbul, TÜRKİYE*
** Sorumlu yazarın e-posta adresi: cemile.bayderedemir@demiroglu.bilim.edu.tr*
DOI: 10.29130/dubited.1552103

ABSTRACT

In the study, the title compound 2-oxo-2-phenylethyl 3-nitroso-2-phenylimidazo[1,2-a]pyridine-8-carboxylate (PIP) was deliberated spectroscopically. Molecular geometry (bond length, bond angle), electronic properties (electronegativity, chemical potential, global hardness, global softness), the highest occupied molecular orbital (HOMO) and the lowest unoccupied molecular orbital (LUMO), Mulliken atomic charge were calculated using the density functional theory DFT/B3LYP method 6−311G++(d,p) level of theory. DFT calculations of the molecular electrostatic potential (MEP), frontier molecular orbitals (FMO), Mulliken charges recognize the chemically active sites of this molecule responsible for its chemical reactivity. The natural bond orbital (NBO) analysis gives an efficient methodology for investigating the inter- and intramolecular bonding, charge transfer and hyperconjugative interactions in molecular systems. TD–DFT calculations were performed at the B3LYP/6–311G++(d,p) level of theory to obtain information about excited states and absorption characteristics.

Keywords: *Imidazo[1,2-a]pyridine, DFT method, HOMO, LUMO energies*

2-okso-2-feniletil 3-nitroso-2-fenilimidazo[1,2-a]piridin-8-karboksilat bileşiğinin DFT çalışmaları

Öz

Bu çalışma da, başlık bileşiği 2-okso-2-feniletil 3-nitroso-2-fenilimidazo[1,2-a]piridin-8-karboksilat (PIP) spektroskopik olarak değerlendirildi. Moleküler geometri (bağ uzunluğu, bağ açısı), elektronik özellikler (elektronegatiflik, kimyasal potansiyel, global sertlik, global yumuşaklık), en yüksek dolu moleküler orbital (HOMO) ve en düşük boş moleküler orbital (LUMO), Mulliken atom yükü, yoğunluk fonksiyonel teorisi DFT/B3LYP yöntemi 6−311G++(d,p) teori seviyesi kullanılarak hesaplandı. Moleküler elektrostatik potansiyel (MEP), sınır moleküler orbitaller (FMO), Mulliken yüklerinin DFT hesaplamaları, bu molekülün kimyasal reaktifliğinden sorumlu kimyasal olarak aktif bölgelerini tanımlar. Doğal bağ orbital (NBO) analizi, moleküler sistemlerde moleküller arası ve molekül içi bağ, yük transferi ve hiperkonjugatif etkileşimlerin araştırılması için etkili bir metodoloji sunar. Uyarılmış durumlar ve absorpsiyon karakteristikleri hakkında bilgi elde etmek için B3LYP/6–311G++(d,p) teori düzeyinde TD–DFT hesaplamaları yapıldı.

Anahtar Kelimeler: *Imidazo[1,2-a]piridin, DFT metodu, HOMO, LUMO enerjileri*

I. INTRODUCTION

Imidazo[1,2-a]pyridines constitute a class of nitrogen-based heterocyclic compounds consisting of the fused of a pyridine moiety to an imidazole ring. A large number of drugs contain N-heterocycles as core structures, including imidazo [1,2-a] pyridine and its derivatives, which are used in medicinal chemistry [1, 2] or exhibit various biological activities such as antibacterial [3], antituberculosis [4], tyrosinase inhibitor [5], HIV inhibitor [6], antidiabetic [7], anti-inflammatory [8] or anticancer activities [9, 10]. A wide range of medications such as Olprinone (for the treatment of acute heart failure), Zolpidem (used in the treatment of insomnia), Miroprofen [11] (used as a analgesic), Zolimidine (used for the treatment of pepticulcer), Minodronic acid [11] (for the treatment of osteoporosis), Saripidem (works as an anxiolytic agent) [12] contain imidazo[1,2-a]pyridine derivatives.

Quantum chemical methods have been veritable tools in determining the molecular structure as well as elucidating the electronic structure and reactivity [13]. Among other methods, the density functional theory (DFT) method has been a very useful method for appraising the structural and spectral properties of organic compounds. This method is based on Kohn-Sham approximation to solve the Schrödinger equation. DFT allows a close connection between theory and experiment and often leads to important clues about the geometric, electronic, and spectroscopic properties of the systems being studied. The goal of a basis set is to provide the best representation of the unknown molecular orbitals (or electron density), with as small a computational cost as possible [14]. Pople and co-workers have introduced a number of basis sets suitable for widespread application of ab-initio molecular orbital theory. These include (i) minimal basis sets, the most popular of which is STO-3G [15] (ii) splitvalence basis sets such as 3-21G, 4-316, and 6-31G [16-18] and (iii) split-valence plus polarization basis sets such as 6-31G* (polarization functions on first-row atoms only) and 6-31G** (polarization functions on hydrogen also) [19]. Pople-type basis sets represented by 6-31G** [18, 20] are widely used as standard basis sets for calculations of large systems because of their reasonable accuracy and computational cost. The literature contains many reports on the successful application of DFT to imidazo[1,2-a]pyridine [21-28].

In this context, the objective of this study is to contribute to the advancement of understanding of the DFT characteristics of substituted imidazo[1,2-a]pyridine derivatives. For this, a series of DFT studies were performed, such as molecular geometric parameters, the highest occupied molecular orbital (HOMO), least unoccupied molecular orbital (LUMO) molecular orbital energy values, molecular electrostatic potential (MEP) map, Mulliken charge analysis, visible ultraviolet light spectrum.

II. MATERIAL AND METHODS

In the present work, a new imidazo[1,2-a]pyridine derivative, 2-oxo-2-phenylethyl 3-nitroso-2-phenylimidazo[1,2-a]pyridine-8-carboxylate ($C_{22}H_{15}N_3O_4$) was synthesized and its structure was determined by X-ray crystallography [29]. Diffraction data of PIP was collected with STOE IPDS 2 diffractometer equipped with graphite monochromatic MoKα radiation (λ= 0.71073) at 296 K [30]. The structure was solved and refined with SHELXT-2018/3 [31] program. Molecular graphics was plotted with Mercury for Windows [32]. For investigating the hydrogen bond in the crystal was used PLATON [33] software. In preparation for publication was used WinGX [34] and PublCIF [35] programs.

DFT calculations were made using the Gaussian 09 package program [36] and the results are shown using Gaussview 5.0 [37] molecular visulation program. The applied method are Becke's [38] three parameter hybrid exchange functional with Lee-Yang- Parr correlation functional [39] method (B3LYP) with 6–311++G (d,p) basis set. TD–DFT calculations at the B3LYP/6–311++G(d,p) level were performed to obtain information about the excited states and absorption characteristics. The natural bond orbital (NBO) calculations [40] were performed using NBO 3.1 program implemented in the Gaussian 09 package [36] at the DFT/B3LYP/6-31G(d,p) method.

By using the energies of Frontier Molecular Orbitals, the ionization energy (IP) and electron affinity (EA) can be determined by the following formulas [41].

$$EA = -E_{LUMO} \quad (1)$$

$$IP = -E_{HOMO} \quad (2)$$

The chemical potential (μ), absolute electronegativity (χ) and absolute hardness (η) were calculated from combination of ionization energy and electron affinity values using the following equations [42]

$$\chi = -\mu = (IP + EA)/2 \quad (3)$$

$$\eta = (IP - EA)/2 \quad (4)$$

and

$$\sigma = 1/\eta \quad (5)$$

denotes the softness (σ).

The electrophilicity index (ω) and its multiplicative inverse i.e. the nucleophilicity index (ε) were calculated using the following formulas [43, 44].

$$\omega = \mu^2/2\eta \quad (6)$$

$$\varepsilon = 1/\omega \quad (7)$$

In the Natural Bond Orbital (NBO) analysis, the hyper-conjugative interaction energy was deduced from the second-order perturbation approach.

$$E^{(2)} = q_i \frac{F^2(i,j)}{\varepsilon_j - \varepsilon_j} \quad (8)$$

where q_i is the donor orbital occupancy, ε_j and ε_i are diagonal elements and F(i, j) is the off diagonal NBO Fock matrix element.

In NMR analysis, the difference between the isotropic magnetic shielding (IMS) of tetramethylsilane (TMS) and proton (x) determines the chemical shift of any "x" proton (X). The following formula defines it:

$\delta X = IMSTMS = - IMSX$

III. RESULTS AND DISCUSSION

A. GEOMETRY OPTIMIZATION

The molecule (PIP) has an imidazole ring, a pyridine ring, and two phenyl rings. The molecular structure of PIP is shown in Figure 1 (a). The optimized geometry of the molecule (PIP) is presented in Figure 1 (b). DFT and XRD studies, optimized structural parameters such as bond length and bond angle are given in Table 1 and Table 2.

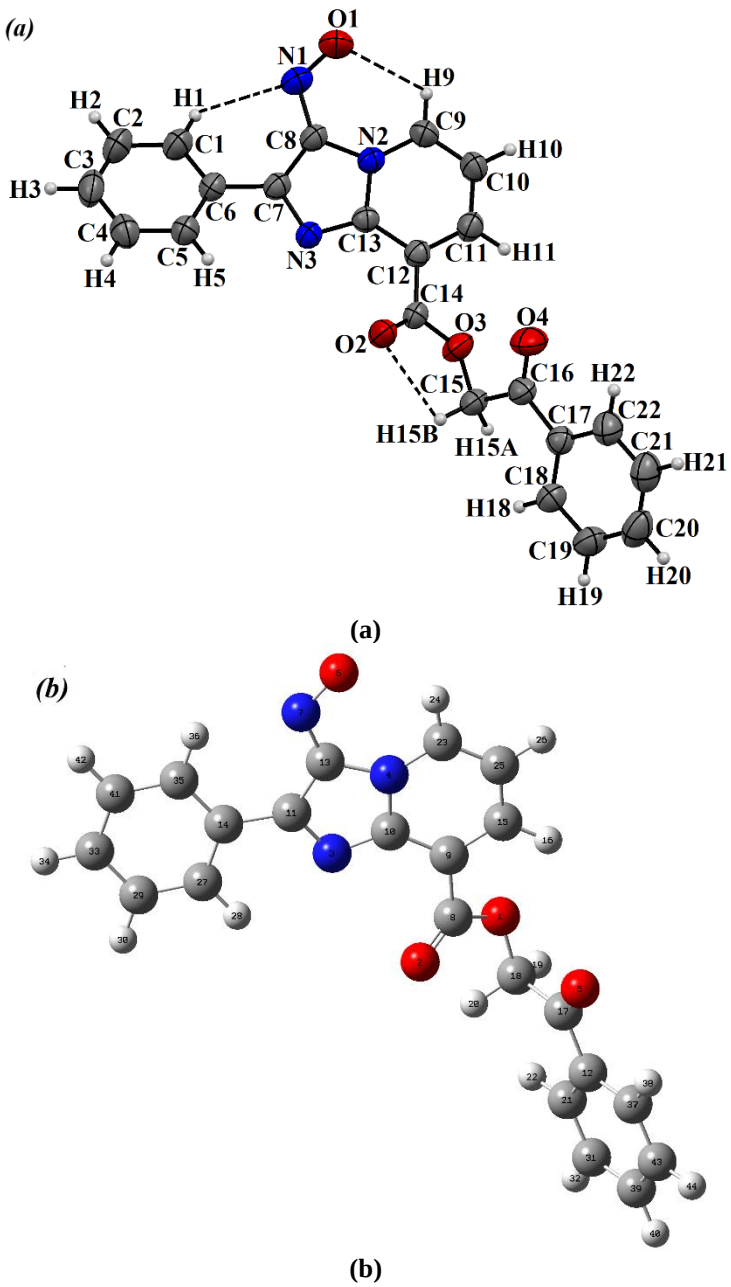

Figure 1. a) *X-Ray crystal structure of the PIP compound,* ***b)*** *optimized geometric structure obtained using B3LYP/6−311++G(d,p) level*

The bond lengths and bond angles of the molecule obtained experimentally from the X-ray structure analysis of the PIP compound and theoretically optimized by DFT/B3LYP/6−311G(d,p) are given in Table 1 and Table 2, respectively.

Table 1. *Experimental and theoretical bond lengths.*

	Experimental	**Theoretical**		**Δ**
Bond length (Å)	**X-ray**	**6−311G++(d,p)**	**6-31G++(d,p)**	
O3−C14	1.3431(16)	1.343	1.343	0.0001
O3−C15	1.4365(16)	1.4364	1.4364	0.0001
O2−C14	1.2018(16)	1.2019	1.2018	-0.0001
N3−C7	1.3491(16)	1.349	1.3491	0.0001
N3−C13	1.3526(16)	1.3526	1.3526	0
N2−C9	1.3729(17)	1.3729	1.3729	0
N2−C13	1.3918(16)	1.3916	1.3919	0.0002
N2−C8	1.4092(16)	1.4093	1.4092	-0.0001
O4−C16	1.2157(17)	1.2159	1.2157	-0.0002
O1−N1	1.2446(16)	1.2446	1.2445	0
N1−C8	1.3732(17)	1.3731	1.3733	0.0001
C14−C12	1.4951(18)	1.495	1.4052	0.0001
C12−C11	1.3783(18)	1.3783	1.3784	0
C12−C13	1.4166(18)	1.4167	1.4165	-0.0001
C7−C8	1.4115(19)	1.4116	1.4115	-0.0001
C7−C6	1.4803(18)	1.4803	1.4802	0
C17−C18	1.390(2)	1.3903	1.3902	-0.0003
C17−C22	1.391(2)	1.3904	1.3906	-0.0004
C17−C16	1.4907(19)	1.4906	1.4908	0.0001
C6−C5	1.387(2)	1.3866	1.3868	0.0004
C6−C1	1.396(2)	1.3961	1.3960	-0.0001
C11−C10	1.4002(19)	1.4002	1.4002	0
C11−H11	0.9300	0.9299	0.9299	0.0001
C16−C15	1.511(2)	1.5106	1.5109	0.0004
C15−H15A	0.9700	0.9703	0.9700	-0.0003
C15−H15B	0.9700	0.9699	0.9700	0.0001
C18−C19	1,381(2)	1,3814	1.3814	-0,0004
C18−H18	0.9300	0.93	0.93	0
C9−C10	1.3581(19)	1.3582	1.3581	-0.0001
C9−H9	0.9300	0.93	0.9301	0
C10−H10	0.9300	0.9299	0.9300	0.0001
C5−C4	1.386(2)	1.3863	1.3861	-0.0003
C5−H5	0.9300	0.9299	0.9300	0.0001
C4−C3	1.380(2)	1.3803	1.3805	-0.0003
C4−H4	0.9300	0.93	0.93	0
C19−C20	1.385(3)	1.3772	1.3844	0.0078
C19−H19	0.9300	0.9299	0.9300	0.0001
C3−C2	1.375(3)	1..3753	1.3753	-0.0003
C3−H3	0.9300	0.93	0.93	0
C1−C2	1.381(2)	1.3805	1.3806	0.0005
C1−H1	0.9300	0.9301	0.9300	-0.0001
C22−C21	1.376(2)	1.376	1.3762	0
C22−H22	0.9300	0.9301	0.9299	-0.0001
C20−C21	1.377(3)	1.376	1.3844	0.0001
C20−H20	0.9300	0.9299	0.9300	0.0001
C2−H2	0.9300	0.9301	0.9300	-0.0001
C21−H21	0.9300	0.9299	0.9299	0.0001

Table 2. *Experimental and theoretical bond angles.*

	Experimental	Theoretical		Δ
Bond angle (Å)	**X-ray**	**6−311G++(d,p)**	**6-31G++(d,p)**	
C14−O3−C15	117.98(11)	117.9746	117.9817	0.0054
C7−N3−C13	105.94(10)	105.9402	105.9449	-0.0002
C9−N2−C13	123.04(11)	123.0446	123.0335	-0.0046
C9−N2−C8	131.29(11)	131.281	131.3003	0.009
C13−N2−C8	105.67(10)	105.6742	105.6661	-0.0042
O1−N1−C8	117.36(12)	117.3547	117.3628	0,0053
O2−C14−O3	124.53(12)	124.5349	124.5381	-0.0049
O2−C14−C12	125.28(12)	125.2799	125.2785	0.0001
O3−C14−C12	110.15(11)	110.1519	110.1498	-0.0019
C11−C12−C13	118.33(11)	118.3246	118.3336	0.0054
C11−C12−C14	120.41(11)	120.415	120.4110	-0.005
C13−C12−C14	120.94(11)	120.9489	120.9337	-0.0089
N3−C13−N2	111.88(10)	111.8815	105.9449	-0,0015
N3−C13−C12	130.17(11)	130.1666	130.1757	0.0034
N2−C13−C12	117.93(11)	117.9311	130.9282	-0.0011
N3−C7−C8	111.24(11)	111.2482	111.2429	-0.0082
N3−C7−C6	121.04(11)	121.0434	121.0462	-0.0034
C8−C7−C6	127.70(11)	127.695	127.6978	0.005
C18−C17−C22	119.06(13)	119.052	119.0586	0.008
C18−C17−C16	122.36(13)	122.357	122.3633	0.003
C22−C17−C16	118.53(13)	118.5445	118.5324	-0.0145
N1−C8−N2	127.33(12)	127.3477	127.3316	-0.0177
N1−C8−C7	127.34(12)	127.3386	127.3378	0.0014
N2−C8−C7	105.26(10)	105.2506	105.2658	0.0094
C5−C6−C1	118.72(13)	121.7281	118.7151	-3.0081
C5−C6−C7	119.55(12)	119.5482	119.5528	0.0018
C1−C6−C7	121.73(13)	121.7281	121.7313	0.0019
C12−C11−C10	121.69(12)	121.6964	121.6887	-0.0064
C12−C11−H11	119.2	119.1538	119.1573	0.0462
C10−C11−H11	119.2	119.1498	119.1540	0.0462
O4−C16−C17	121.74(14)	121.7382	121.7421	0.0018
O4−C16−C15	118.84(13	118.8188	118.8380	0.0212
C17−C16−C15	119.41(12)	119.4364	119.4129	-0.0264
O3−C15−C16	108.54(11)	108.5589	108.5364	-0.0189
O3−C15−H15A	110.0	109.9747	109.9875	0.0253
C16−C15−H15A	110.0	109.9626	109.9785	0.0374
O3−C15−H15B	110.0	109.9975	109.9909	0.0025
C16−C15−H15B	110.0	110.0098	109.9877	-0.0098
H15A−C15−H15B	108.4	108.3333	108.3558	0.0667
C19−C18−C17	119.98(15)	119.9894	119.9824	-0.0094
C19−C18−H18	120.0	119.813	120.0121	-0.0017
C17−C18−H18	120.0	120.0017	120.0055	-0.0017
C10−C9−N2	118.84(12)	118.8332	118.8384	0.0068
C10−C9−H9	120.6	120.5765	120.5840	0.0235
N2−C9−H9	120.6	120.5904	120.5776	0.0096
C9−C10−C11	120.11(13)	120.1041	120.1115	0.0059
C9−C10−H10	119.9	119.9461	119.9425	-0.0461
C11−C10−H10	119.9	119.9498	119.9460	-0.0498
C4−C5−C6	120.80(14)	120.7907	120.8041	0.0093
C4−C5−H5	119.6	119.6021	119.6016	-0.0021
C6−C5−H5	119.6	119.6072	119.5943	-0.0072

C3−C4−C5	119.83(15)	119.8396	119.8343	-0.0096
C3−C4−H4	120.1	120.0884	120.0825	0.0116
C5−C4−H4	120.1	120.072	120.0832	0.028
C18−C19−C20	120.37(16)	120.3628	120.3755	0.0072
C18−C19−H19	119.8	119.8242	119.8098	-0.013
C20−C19−H19	119.8	119.813	119.8147	-0.013
C2−C3−C4	119.82(14)	119.825	119.8248	-0.005
C2−C3−H3	120.1	120.0793	120.0845	0.0207
C4−C3−H3	120.1	120.0957	119.6292	0.0043
C2−C1−C6	120.06(16)	120.0619	120.0636	-0.0019
C2−C1−H1	120.0	119.9804	119.9728	0.0196
C21−C22−C17	120.64(16)	120.6594	120.6379	-0.0194
C21−C22−H22	119.7	119.6693	119.6867	0.0307
C17−C22−H22	119.7	119.6713	119.6754	0.0287
C21−C20−C19	119.80(15)	120.1272	119.7980	-0.3272
C21−C20−H20	120.1	119.957	120.0978	0.143
C19−C20−H20	120.1	120.0938	120.1042	0.0062
C3−C2−C1	120,74(15)	120,7402	120.7382	-0,0032
C3−C2−H2	119.6	119.630	119.6292	-0.03
C1−C2−H2	119.6	119.6298	119.6326	-0.0298
C22−C21−C20	120.14(17)	120.1272	120.1384	0.0128
C22−C21−H21	119.9	119.957	119.9278	-0.057
C20−C21−H21	119.9	119.9158	119.9338	-0.0158

The selected DFT optimization and metrical parameters from X-ray diffraction are tabulated in Table 1 and Table 2. It is understood from the results given in Table 1 and Table 2 that, experimental and theoretical data are in good agreement with each other. The negligible differences between the experimental and calculated bond lengths and angles are due to the fact that the computations were performed and calculated in the gas phase, while the X-ray data were obtained in the solid phase. The maximum difference between experimental and theoretical bond lengths was determined as 0.0078 Å between C19−C20 atoms, and the maximum difference between bond angles was determined as -0.3272° between C21−C20−C19 atoms. The bond length C19−C20 in the molecule was observed as 1.385(3) Å and the same bond length was calculated as 1.3844 and 1.3772 Å for 6–31G++(d, p) and 6–311G++(d, p) basis sets. As a result, the fact that the error margin in the calculations was quite low showed that the DFT/B3LYP/6−311G++(d,p) method can be used in the characterization of the three-dimensional structure of the molecular geometries of Imidazo [1,2-a] pyridine derivative compounds in similar studies.

B. FRONTİER MOLECULAR ORBITAL ANALYSIS

The HOMO (highest occupied molecular orbital) acts as an electron donor and the LUMO (lowest occupied molecular orbital) as an electron acceptor. When the energy gap is small, the molecule is highly polarizable and has high chemical reactivity. The energy levels, energy gaps, hardness (η), softness (σ) and electronegativity (χ) are given in Table 3. The electron transition from the HOMO to the LUMO energy level is shown in Figure 2. The chemical hardness and softness of a molecule is a sign of its chemical stability. From the HOMO–LUMO energy gap, we can see whether or not the molecule is hard or soft. If the energy gap is large, the molecule is hard and if small the molecule is soft. Soft molecules are more polarizable than hard ones because they need less energy for excitation.

Table 3. *Quantum molecular descriptors of the compound* $C_{22}H_{15}N_3O_4$.

FMO	Energy (eV)
E_{HOMO}	-6.0034
E_{LUMO}	-2.7810

Energy difference (ΔE)	3.2224
Ionization Potential (IP)	6.0034
Electron Affinity (EA)	2.7810
Chemical Potential (μ)	-4.3922
Electronegativity (χ)	4.3922
Global Hardness (η)	1.6112
Global Softness (σ)	0.3103

Based on the numerical values collated in Table 3, the title compound can be classified as a hard material with a HOMO–LUMO energy gap of 3.2224 eV.

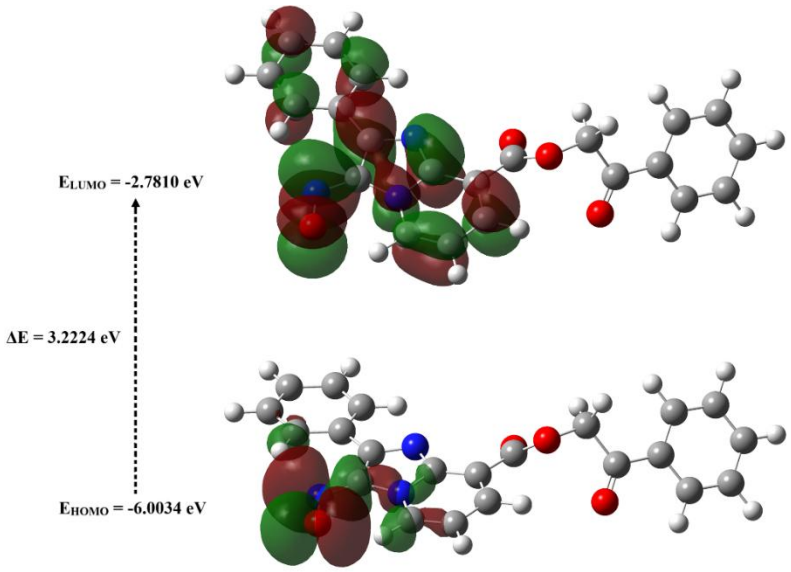

Figure 2*. Three-dimensional representation and energy values of the occupied and empty molecular orbitals of the* $C_{22}H_{15}N_3O_4$ *molecule.*

C. MOLECULAR ELECTROSTATIC POTENTIAL (MEP)

Molecular electrostatic potential (MEP) displays molecular size and shape as well as positive, negative and neutral electrostatic potential regions in terms of colour grading and is useful in investigating relationships between molecular structure and physicochemical properties [45]. The MEP map (Figure 3) was calculated at the B3LYP/6-311 G++(d,p) level of theory. The red and blue-coloured regions indicate nucleophiles (electron rich) and electrophile regions (electron poor), respectively. The white regions indicate neutral atoms. In the title molecule, the red regions are concentrated at the carbonyl group. It possesses the most negative potential and is thus the strongest repulsion site (electrophilic attack). The blue regions indicate the strongest attraction regions, which are occupied mostly by hydrogen atoms.

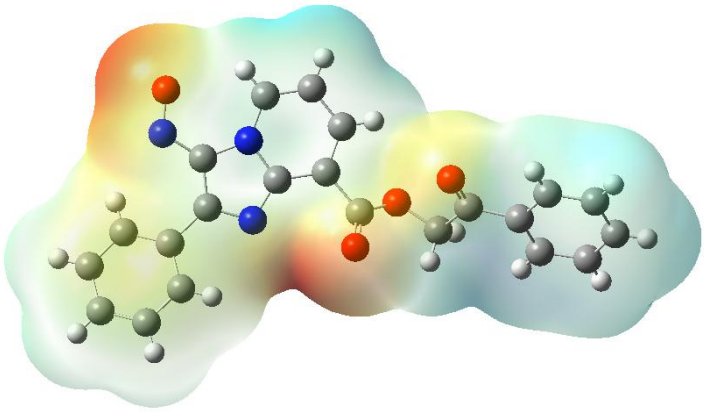

Figure 3. *MEP surface of* $C_{22}H_{15}N_3O_4$ *molecule.*

D. EXAMINATION OF MULLIKEN'S CHARGE

Mulliken atomic charge calculation has an important role for the application of quantum chemical calculations of the molecular system. Atomic charge affects dipole moment, polarizability, electronic structure and other properties of a molecular system [46].
The results calculated with the 6−311G++(d,p) basis set in the Mulliken density analysis DFT/B3LYP method to calculate the atomic charges of the PIP molecule are listed in Table 4.

Table 4. *Calculated Mulliken charge of* $C_{22}H_{15}N_3O_4$.

Atoms	B3LYP/6-311G++(d,p)
O1	0.086102
O2	-0.145763
N3	0.102607
N4	0.119621
O5	-0.195024
O6	-0.004001
N7	-0.314148
C8	-0.827447
C9	0.868358
C10	-0.032332
C11	0.761205
C12	1.420419
C13	-0.719964
C14	1.195501
C15	-0.394814
C17	-0.060600
C18	-0.112647
C21	-1.435191
C23	0.166112
C25	-0.802156
C27	0.061925
C29	-0.399728
C31	-0.466708
C33	-0.176385
C35	-0.818374
C37	0.530548
C39	-0.217663
C41	-0.261100

C43	-0.297953

When these results are examined, positive charges are collected on the atoms O1, N3, N4, C9, C11, C12, C14, C23, C27, C37 in the PIP molecule. Negative charges are collected on all other atoms.

E. VISIBLE ULTRAVIOLET LIGHT (UV-VIS) ANALYSIS

The calculated electronic absorption spectrum of the compound PIP was calculated by TD-DFT at the B3LYP/6–311G++(d,p) level. The visible ultraviolet light spectrum of the 2-oxo-2-phenylethyl 3-nitroso-2-phenylimidazo[1,2-a]pyridine-8-carboxylate compound is shown in Figure 4. Table 5 summarizes the theoretical maximum absorption wavelengths (λ_{max}), excitation energy (E), oscillator strengths (f_{os}) and major transitions of the investigated compound.

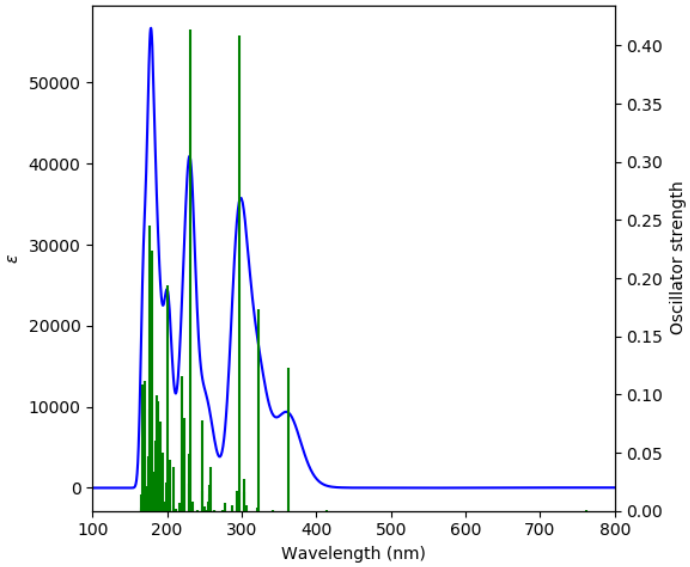

Figure 4. *Visible ultraviolet light spectrum of the title molecule*

Table 5. *Excitation energy (cm^{-1}), oscillator strengths (f_{os}) and maximum absorption wavelengths (λ_{max}/nm) of the PIP molecule*

λ(nm)	**E(cm^{-1})**	**f**	**Major contributions (>%10)**
362.42	27592	0.123	H-2→LUMO (%46), H-1→LUMO (%43)
322.68	30990	0.1732	H-1→LUMO (%35), H-1→L+2 (%44)
297.20	33648	0.4084	H-2→LUMO (%19), H-2→L+2 (%21), H-1→LUMO (%11), H-1→L+2 (%28)
231.87	43128	0.4142	H-7→L+1 (%46), H-6→L+1 (%28)
219.78	45501	0.116	H-3→L+4 (%23), H-1→L+4 (%32), H-1→L+6 (%17)
200.94	49766	0.1944	H-11→LUMO (%17), H-2→L+5 (%40), H-1→L+5 (%15)
180.45	55416	0.2233	H-11→L+2 (%37), H-9→L+4 (%13), H-3→L+6 (%10)
177.46	56351	0.245	H-7→L+3 (%30), H-6→L+3 (%21)
170.51	58646	0.1119	H-18→LUMO (%28), H-14→L+2 (%15), H-8→L+5 (%11)
167.18	59815	0.1086	H-18→LUMO (%33), H-9→L+4 (%10), H-8→L+4 (%14)

The calculated maximum absorption wavelengths are 362.42, 322.68, 297.20, 231.87, 219.78, 200.94, 180.45, 177.46, 170.51 and 167.18 nm. The oscillator strengths corresponding to these values are 0.123, 0.1732, 0.4084, 0.4142, 0.116, 0.1944, 0.2233, 0.245, 0.1119 and 0.1086. These values indicate more intense permitted transitions.

F. NATURAL BOND ORBİTAL ANALYSİS

Natural Bond Orbital (NBO) approach expressed by $E^{(2)}$, an energy from the second-order perturbation is an analytical method for examining intra and intermolecular bonding. The NBO analysis provides a simple foundation for studying charge transfer or hyperconjugative interactions. This analysis enables study of interactions between filled Lewis type donor and empty non-Lewis acceptor orbitals. The most efficient interactions between the Lewis-type occupied NBO orbital (bonding) with non-Lewis unoccupied NBO orbital (anti-bonding) are listed in Table 6.

Table 6. *Selected Second Order Perturbation Theory Analysis of Fock Matrix in NBO Basis ($E^{(2)}$ > 20 kcal/mol) of the title compound.*

Type	Donor	Acceptor	$E^{(2)}$ (kcal/mol)	Ej-Ei (a.u.)	F_{ij} (a.u.)
σ-σ*	N4-C10	C23-C25	21.02	0.37	0.079
σ-σ*	C9-C15	N4-C10	33.11	0.20	0.081
σ-n	C11-C13	N3	56.21	0.09	0.085
σ-σ*	C11-C13	O6-N7	43.14	0.20	0.084
σ-σ*	C12-C21	O5-C17	20.81	0.26	0.069
σ-σ*	C12-C21	C37-C43	19.97	0.29	0.070
σ-σ*	C14-C27	C11-C13	20.66	0.23	0.064
σ-σ*	C14-C27	C35-C41	20.60	0.28	0.070
σ-σ*	C23-C25	C9-C15	20.73	0.31	0.071
σ-σ*	C29-C33	C14-C27	22.06	0.29	0.071
σ-σ*	C31-C39	C12-C21	22.90	0.28	0.072
σ-σ*	C35-C41	C29-C33	22.65	0.28	0.072
σ-σ*	C37-C43	C12-C21	20.43	0.28	0.068
σ-σ*	C37-C43	C31-C39	22.73	0.28	0.072
n-σ*	O1	O2-C8	43.32	0.34	0.109
n-σ*	O2	O1-C8	36.48	0.60	0.135
n-σ*	O2	C8-C9	20.37	0.67	0.107
n-σ*	N3	N4-C10	184.60	0.10	0.126
n-σ*	N3	C11-C13	80.18	0.18	0.116
n-σ*	O5	C17-C18	21.52	0.64	0.106
σ*-σ*	N4-C10	C9-C15	53.05	0.09	0.088
σ*-σ*	N4-C10	C23-C25	27.05	0.08	0.061
σ*-σ*	O5-C17	C12-C21	63.06	0.03	0.072
σ*-σ*	O6-N7	C11-C13	40.83	0.07	0.075
σ*-σ*	C11-C13	C14-C27	44.94	0.05	0.066
σ*-σ*	C12-C21	C37-C43	266.86	0.01	0.083

As can be seen from this table 6, NBO analysis revealed that the n(N3)→ σ*(N4–C10), σ*(C12–C21)→σ*(C37–C43) interactions give a strong stabilization to the system of the title compound by 184.60 kcal/mol, 266.86 kcal/mol respectively. The other primary hyperconjugative interactions lone pair NBO orbitals of n(O1)→ σ*(O2–C8), n(O2)→ σ*(O1–C8), n(O2)→ σ*(C8–C9), n(O5)→ σ*(C17–C18) and n(N3)→ σ*(C11–C13) are stabilized to the molecule up to 43.32, 36.48, 20.37, 21.52 and 80.18 kcal/mol, respectively. A few essential hyperconductivity interactions between bonding to antibonding σ-σ∗ orbitals are σ(C11–C13) →σ∗(O6–N7) with a stabilization energy value of 43.14 kcal/mol.

F. NMR SPECTRAL STUDİES

Nuclear magnetic resonance spectroscopy, most commonly known as NMR spectroscopy is one of the most essential techniques for determining the structure of organic compounds. In this study, The theoretical ^{13}C and ^{1}H chemical transformations are calculated for the optimal geometry using the

standard Gauge Invariant Atomic Orbital (GIAO) method [47]. The theoretical NMR chemical shifts are given in Table 7.

Table. 7. *The theoretical ^{1}H and ^{13}C NMR Chemical Shifts in ppm*

H-atom	B3LYP	C-atom	B3LYP
H-24	7.09	C-17	199.15
H-36	6.85	C-11	168.66
H-28	6.39	C-8	166.29
H-38	6.02	C-13	162.50
H-16	5.85	C-10	149.07
H-22	5.55	C-12	137.41
H-34	5.45	C-14	137.05
H-30	5.37	C-15	135.51
H-40	5.36	C-35	131.87
H-44	5.28	C-39	129.42
H-42	5.22	C-23	128.33
H-32	5.17	C-27	128.23
H-26	4.55	C-9	127.70
H-20	2.99	C-37	126.53
H-19	2.11	C-33	126.40
		C-43	125.21
		C-29	124.66
		C-31	124.36
		C-41	123.62
		C-21	123.55
		C-25	114.18
		C-18	58.87

In ^{13}C NMR spectra (Figure 5), the resonance signals of the carbonyl group (C=O) were obtained a theoretically at 199.15 and 166.29 ppm. The chemical shifts of the carbons present in the pyrimidine ring are found computed data at 168.66 and 162.50 ppm. The carbon at the junction (N−C=N) was theoretically found at 149.07 ppm. The signals at 137.41, 129.42, 126.53, 125.21, 124.36 and 123.55 ppm in the theoretical spectrum are assigned to the carbons of the phenyl ring. Additionally, the other phenyl ring carbons appeared at 137.05, 131.87, 128.23, 126.40, 124.66 and 123.62 ppm.

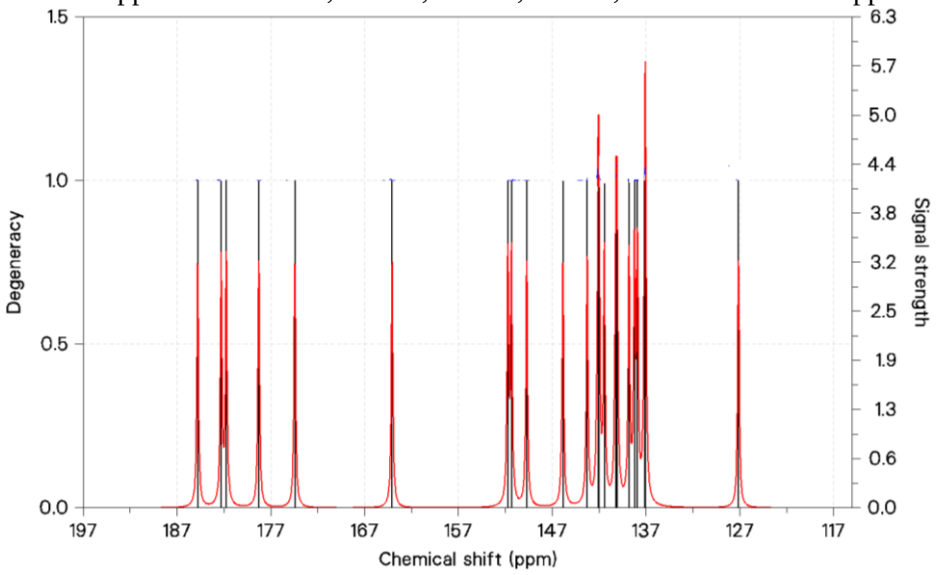

Figure 5*. ^{13}C NMR spectrum of title molecule.*

In ^{1}H NMR spectra (Figure 6), the title compound contains one set of aromatic protons in the region δ4.55−7.09 and a set of aliphatic protons in the region δ2.11− 2.99.

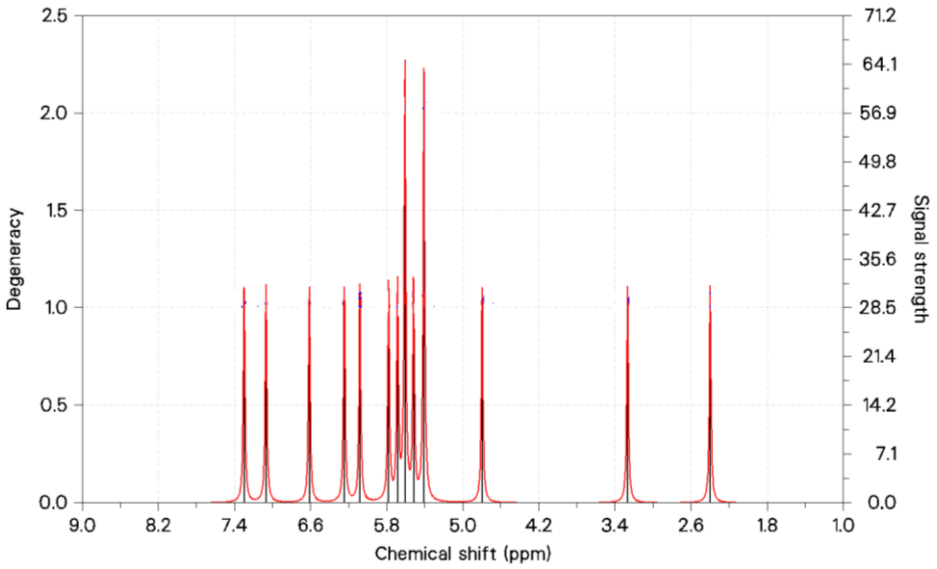

Figure 6. *^{1}H NMR spectrum of title molecule.*

IV. RESULTS

Quantum chemical computations were carried out using DFT at B3LYP/6–311G++(d, p) level of theory and the optimized parameters were investigated to predict and to understand their reactivity and behavior. The optimal structure was calculated using DFT and compared with the single crystal structure, and the results were consistent. Moreover, the physicochemical properties of the title compound were further clarified by the analysis of MEP, FMOs and NBO. The energy gap (ΔE) between the HOMO and LUMO molecular orbitals was obtained as 3.2224 eV. This value shows that the molecule has a low tendency to react chemically and that the molecule has a stable structure. The predicted MEP surface reveals potential nucleophilic and electrophilic sites for chemical interactions. Notably, the negative electrostatic potential region is prominently concentrated around O1 and O2, indicating the presence of nucleophilic centers in this region. The Mulliken atomic charges of the molecule were calculated and it was found that the carbonyl group and the nitrogen atom inductively withdraw electrons. The NBO analysis indicated the intra and intermolecular charge transfer between the bonding and antibonding orbitals. From NBO analysis it is observed that for the title compound n(N3)→σ*(N4–C10), σ*(C12–C21)→σ*(C37–C43) interaction has highest stabilization energy of 184.60 kcal/mol, 266.86 kcal/mol, respectively.

Finally, according to the theoretical data, the title molecule has high potential for application value in the pharmaceutical and chemical fields.

ACKNOWLEDGEMENT: This work is supported by Ondokuz Mayıs University Scientific Project (project no: PYO FEN.1906.19.001).

Article Information

Acknowledgments: The author expresses her sincere thanks to the editor and anonymous referees for their helpful comments and suggestions.

Author's Contributions: Authors 1: Writing, original draft, review, analysis and editing.

Artificial Intelligence Statement: No any Artificial Intelligence tool is used in this paper.

Conflict of Interest Disclosure: No potential conflict of interest was declared by authors.

Plagiarism Statement: This article was scanned by the plagiarism program.

V. REFERENCES

[1] T. Swainston Harrison and G. M. Keating, "Zolpidem: a review of its use in the management of insomnia," *CNS Drugs*, vol. 19, pp. 65–89, 2005.

[2] A. Deep et al., "Imidazo[1,2-a]pyridine scaffold as prospective therapeutic agents," *Current Topics in Medicinal Chem*istry, vol. 17, no. 2, pp. 238–250, 2017.

[3] N. P. Mishra et al., "Design, one-pot synthesis, molecular docking study, and antibacterial evaluation of novel 2H-chromene based imidazo[1,2-a]pyridine derivatives as potent peptide deformylase inhibitors," *Journal of Molecular Structure*, vol. 1246, 2021, Art. no. 131183.

[4] A. Wang et al., "Design, synthesis and biological activity of N-(2-phenoxy)ethyl imidazo[1,2-a]pyridine-3-carboxamides as new antitubercular agents," *European Journal of Medicinal Chemistry*, vol. 178, pp. 715–725, 2019.

[5] T. Damghani et al., "Design, synthesis, in vitro evaluation and molecular docking study of N'-Arylidene imidazo[1,2-a]pyridine -2-carbohydrazide derivatives as novel Tyrosinase inhibitors," *Journal of Molecular Structure*, vol. 1222, 2020, Art. no.128876.

[6] M. L. Bode et al., "Imidazo[1,2-a]pyridin-3-amines as potential HIV-1 non-nucleoside reverse transcriptase inhibitors," *Bioorganic & Medicinal Chemistry*, vol. 19, pp. 4227–4237, 2011.

[7] M. Saeedi et al., "Synthesis of 4-alkylaminoimidazo[1,2-a]pyridines linked to carbamate moiety as potent α-glucosidase inhibitors," *Molecular Diversity*, vol. 25, pp. 2399–2409, 2021.

[8] G. B. Gundlewad, S. S. Wagh and B. R. Patil, "Catalyst and Solvent Free Synthesis and Biological Activities of Imidazo[1,2-a]pyridine," *Asian Journal of Organic Medicinal Chemistry*, vol. 5, pp. 221–226, 2020.

[9] Y. N. Yu et al., "Design, Synthesis, and Biological Evaluation of Imidazo[1,2-a]pyridine Derivatives as Novel PI3K/mTOR Dual Inhibitors," *Journal of Medicinal Chemistry*, vol. 63, pp. 3028–3046, 2020.

[10] D. K. Sigalapalli et al., "Synthesis and biological evaluation of novel imidazo[1,2-a]pyridine-oxadiazole hybrids as anti-proliferative agents: Study of microtubule polymerization inhibition and DNA binding," *Bioorganic & Medicinal Chemistry*, vol. 43, 2021, Art. no. 116277.

[11] A. K. Bagdi, S. Santra, K. Monir and A. Hajra, "Synthesis of imidazo[1,2-a]pyridines: a decade update," *Chemical Communications*, vol. 51, pp. 1555-1575, 2015.

[12] V. Kurteva, "Recent Progress in Metal-Free Direct Synthesis ofImidazo[1,2-a]pyridines," *ACS Omega*, vol. 6, pp. 35173-35185, 2021.

[13] E. Kraka and D. Cremer, "Computer design of anticancer drugs," *Journal of the American Chemical Society*, vol. 122, pp. 8245–8264, 2000.

[14] F. Jensen, “Atomic orbital basis sets,” *Wiley Interdisciplinary Reviews: Computational Molecular Science*, vol. 3, no. 3, pp. 273–295, 2012.

[15] W. J. Hehre, R. F. Stewart and J. A. Pople, “ Self-Consistent Molecular-Orbital Methods. I. Use of Gaussian Expansions of Slater-Type Atomic Orbitals,” *Journal of Chemical Physics*, vol. 51, no. 6, pp. 2657-2664, 1969.

[16] J. S. Binkley, J. A. Pople and W. J. Hehre, “ Self-consistent molecular orbital methods. 21. Small split-valence basis sets for first-row elements,” *Journal of the American Chemical Society*, vol. 102, no. 3, pp. 939-947, 1980.

[17] R. Ditchfield, W. J. Hehre and J. A. Pople, “Self-Consistent Molecular-Orbital Methods. IX. An Extended Gaussian-Type Basis for Molecular-Orbital Studies of Organic Molecules,” *Journal of Chemical Physics*, vol. 54, no. 2, pp. 724-728, 1971.

[18] W. J. Hehre, R. Ditchfield and J. A. Pople, “Self—Consistent Molecular Orbital Methods. XII. Further Extensions of Gaussian—Type Basis Sets for Use in Molecular Orbital Studies of Organic Molecules,” *Journal of Chemical Physics*, vol. 56, no. 5, pp. 2257-2261, 1972.

[19] P. C. Hariharan and J. A. Pople, “The influence of polarization functions on molecular orbital hydrogenation energies,” *Theoretica Chimica Acta*, vol. 28, pp. 213-222, 1973.

[20] J. D. Dill and J. A. Pople, “Self-consistent molecular orbital methods. XV. Extended Gaussian-type basis sets for lithium, beryllium, and boron,” *Journal of Chemical Physics*, vol. 62(7), pp. 2921-2923, 1975.

[21] H.A. Khamees et al., “ Crystal structure, DFT calculation, Hirshfeld surface analysis and energy framework study of 6-bromo-2-(4-bromophenyl)imidazo[1,2-a]pyridine,” *Acta Crystallographica Section*, E75, pp. 1620-1626, 2019.

[22] A. E. Aatiaoui et al., “Experimental and theoretical study of new Schiff bases based on Imidazo[1,2-a]pyridine as corrosion inhibitor of mild steel in 1M HCl,” *Journal of Molecular Structure*, vol. 1226, 2021, Art. no. 129372.

[23] D. Chen, Y. Chen, Q. Wu, X. Zhang, W. Liao and Z. Zhou, “Synthesis, crystal structure and vibrational properties of N-(8-(3-(3-(tert-butyl)ureido)phenyl)imidazo[1,2-a]pyridin-6-yl)acetamide,” *Journal of Molecular Structure*, vol. 1245, 2021, Art. no. 131101.

[24] H. Chen, Y. Wang, Q. Liu, Y. Guo, S. Cao and Y. Zhao, “Synthesis and Evaluation of Photophysical Properties of C-3 Halogenated Derivatives of 2-Phenylimidazo[1,2-a]pyridine,” *Chinese Journal of Chemistry*, vol. 40, pp. 2313-2328, 2022.

[25] S. Wang et al., “Synthesis, crystal structure and vibrational properties studies of (S)-N-(1-phenylethyl)-6-(4-(trifluoromethoxy)phenyl)imidazo[1,2-a]pyridine-2-carboxamide,” *Journal of Molecular Structure*, vol. 1272, 2023, Art. no. 134175.

[26] M. Azzouzi et al., “Design, synthesis, and computational studies of novel imidazo[1,2-a]pyrimidine derivatives as potential dual inhibitors of hACE2 and spike protein for blocking SARS-CoV-2 cell entry,” *Journal of Molecular Structure*, vol.1285, 2023, Art. no.135525.

[27] M. Azzouzi et al., “Synthesis, Characterizations and Quantum Chemical Investigations on Imidazo[1,2-a]pyrimidine-Schiff Base Derivative: (E)-2-Phenyl-N-(thiophen 2ylmethylene)imidazo[1,2-a]pyrimidin-3-amine,” *ACS Omega*, vol. 9, pp. 837–857, 2024.

[28] W. Song, L. Li, L. Ma, Z. Yang, Z. Zheng and Z. Zhou, "Synthesis, crystal structure, DFT, vibrational properties, Hirshfeld surface and antitumor activity studies of a new compound 2-(2-chloro-6-(m-tolyl)imidazo[1,2-a]pyridin-3-yl)-N,N-diethylacetamide," *Journal of Molecular Structure*, vol. 1307, 2024, Art. no. 138052.

[29] F. E. Kalai, C. Baydere, N. Dege, A. Abudunia, N. Benchat and K. Karrouchi, "Crystal structure and Hirshfeld surface analysis of 2-oxo-2-phenylethyl 3-nitroso-2-phenylimidazo-[1,2-a]pyridine-8-carboxylate," *Acta Crystallographica Section*, E78, pp. 322-325, 2022.

[30] S. Cie, "X-area (Version 1.18) and X-Red 32, version 1.04", STOE & Cie GmbH, Darmstadt Germany, 2004.

[31] G. M. Sheldrick, "SHELXT: integrating space group determination and structure solution," *Acta Crystallographica Section A: Foundations and Advances*, vol. 70, 2014, Art. no. C1437.

[32] C. F. Macrae et al., "Mercury CSD 2.0-new features for the visualization and investigation of crystal structures," *Journal of Applied Crystallography*, vol. 41, pp. 466–470, 2008.

[33] A. Spek, "Single-crystal structure validation with the program PLATON," *Journal of Applied Crystallography*, vol. 36, pp. 7–13, 2003.

[34] L. J. Farrugia, "WinGX suite for small-molecule single-crystal crystallography," *Journal of Applied Crystallography*, vol. 32, pp. 837–838, 1999.

[35] S. P. Westrip, "publCIF: software for editing, validating and formatting crystallographic information files," *Journal of Applied Crystallography*, vol. 43, pp. 920–925, 2010.

[36] M. J. Frisch et al. "Gaussian 09, Revision D.01", Gaussian, Inc., Wallingford CT, 2013.

[37] R. Dennington, T. Keith and J. Millam, "GaussView, Version 5", Gaussian Inc., Wallingford CT, 2009.

[38] A. D. Becke, "Density-functional exchange-energy approximation with correct asymptotic behavior," *Physical Review A*, vol. 38 no. 6, pp. 3098-3100, 1988.

[39] C. Lee, W. Yang and R. G. Parr, "Development of the Colle-Salvetti correlation-energy formula into a functional of the electron density," *Physical Review B*, vol. 37, pp. 785–789, 1988.

[40] E. D. Glendening, A. E. Reed, J. E. Carpenter and F. Weinhold, "NBO, Version 3.1", Theoretical Chemistry Institute, University of Wisconsin, Madison, 1998.

[41] N. Islam and S. Kaya, *Conceptual Density Functional Theory and its Application in the Chemical Domain*, USA and Canada: Apple Academic Press Inc., 2018.

[42] N. A. Ancın, S. G. Öztaş, Ö. Küçükterzi and N. A. Öztaş¸ "Theoretical investigation of Ntrans cinnamylidene-m-toluidine by DFT method and molecular docking studies," *Journal of Molecular Structure*, 1198, 2019, Art. no. 126868.

[43] P. K. Chattaraj and D. R. Roy, "Update 1 of: Electrophilicity Index," *Chemical Reviews*, vol. 107, no. 9, pp. 46-74, 2007.

[44] R. G. Parr, L. v Szentpaly and S. Liu, "Electrophilicity index," *Journal of the American Chemical Society*, vol. 121, pp. 1922-1924, 1999.

[45] E. Scrocco and J. Tomasi, “Electronic molecular structure, reactivity and ıntermolecular forces: an euristic interpretation by means of electrostatic molecular potentials,” in *Advances in Quantum Chemistry*, vol. 11, P. O. Löwdin, Ed., New York, NY, USA: Academic Press, 1978, pp. 115–193.

[46] K. Parimala and V. Balachandran, “Structural study, NCA, FT-IR, FT-Raman spectral investigations, NBO analysis and thermodynamic properties of 2', 4'- difluoroacetophenone by HF and DFT calculations,” *Spectrochimica Acta*, vol. 110, pp. 269–284, 2013.

[47] P. G. Patil et al., “Synthesis, Structural Characterizations and Quantum Chemical Investigations on 1-(3-Methoxyphenyl)-3-naphthalen-1-yl-propenone,” *ACS Omega*, vol. 6, pp. 25982−25995, 2021.